

Ponded infiltration in a grid of permanent single-ring infiltrometers: Spatial versus temporal variability

Jana Votrubova^{1*}, Michal Dohnal¹, Tomas Vogel¹, Miroslav Tesar², Vladimira Jelinkova³,
Milena Cislerova¹

¹ Czech Technical University in Prague, Faculty of Civil Engineering, Thákurova 7, 166 29 Prague 6, Czech Republic.

² Institute of Hydrodynamics of the Czech Academy of Sciences, Pod Pařankou 5, 166 12 Prague 6, Czech Republic.

³ Czech Technical University in Prague, University Centre for Energy Efficient Buildings, Trinecká 1024, 273 43 Buštěhrad, Czech Republic.

* Corresponding author. Tel.: +420 22435 4355. E-mail: jana.votrubova@fsv.cvut.cz

Abstract: Temporal variability of the soil hydraulic properties is still an open issue. The present study deals with results of ponded infiltration experiments performed annually in a grid of permanent measurement points (18 spatial and 14 temporal replicates). Single ring infiltrometers were installed in 2003 at a meadow site in the Bohemian Forest highlands, the Czech Republic. The soil at the plot is coarse sandy loam classified as oligotrophic Eutric Cambisol. Soil water flow below infiltration rings has distinctly preferential character.

The results are marked with substantial interannual changes of observed infiltration rates. Considering just the results from the initial four years of the study, the temporal variability did not exceed the spatial variability detected in individual years. In later years, a shift to extremely high infiltration rates was observed. We hypothesize that it is related to structural changes of the soil profile possibly related to combined effect of soil biota activity, climatic conditions and experimental procedure. Interestingly, the temporal changes can partly be described as fluctuations between seemingly stable infiltration modes. This phenomenon was detected in the majority of rings and was found independent of the initial soil moisture conditions.

Keywords: Soil infiltrability; Infiltration instability; Infiltration modes; Burrowing animals; Preferential flow.

INTRODUCTION

The infiltration of rainwater into soil is an important component of hydrological cycle responsible for replenishing soil moisture and groundwater reservoirs (e.g., Gomi et al., 2008). Infiltration rate determines the amounts of surface runoff during heavy rains and rapid snowmelt events. Soil profile ability to take in water is often evaluated using soil infiltrability (also referred to as potential infiltration rate), i.e. infiltration under unlimited water supply. The soil infiltrability can be measured by laboratory or field ponded infiltration experiments.

Field ponded infiltration experiments are usually performed in a single- or double-ring configuration. The choice of the more experimentally demanding double-ring configuration is usually justified by the assumption of nearly one-dimensional character of water flow below the inner ring, which, however, has been many times questioned (e.g., Dohnal et al., 2016; Dusek et al., 2009; Šimůnek, 1988). The single-ring configuration is experimentally simpler with considerably easier installation and lower water consumption; fully developed three-dimensional water flow can be assumed.

No single method is satisfactory for all field conditions (Johnson, 1963). Conducting and evaluating a ponded infiltration experiment in soils with natural structure is accompanied by a large number of complications, most importantly the disturbance of soil around ring walls during ring insertion, the intricate role of vegetation cover, and the limited representativeness of the determined values for the experimental site of interest. A number of experimental problems are related to the process of the ring insertion and the selection of the location. Hence, when studying the temporal variability of the infiltration rate it is sometimes recommended to carry out the infiltration experiments in a grid of permanent infiltration rings. Bagarello and Sgroi (2004) recommended installing the rings a few

months before starting the infiltration experiments to reduce the influence of the small-scale variability of hydraulic conductivity on the data collected at different times and to improve their representativeness at the field scale.

In general, soil hydraulic properties significantly vary with time (Angulo-Jaramillo et al., 1997; Hu et al., 2009) as well as with the spatial coordinate (Ferreira et al., 2015). Time changes of surface hydraulic properties are frequently studied in agricultural fields, including changes associated with disturbance of surface layer by soil cultivation (Kargas et al., 2016; Starr, 1990) or plant growth (Ma et al., 2009). Studies dealing with spatial variability of infiltration in natural catchments are rather rare (e.g., Sharma et al., 1980).

Based on changes in final infiltration rates between two subsequent ponded infiltrations at ryegrass meadow in the Bohemian Forest, Czech Republic, Cislerova et al. (1988) speculated that entrapped air alters the volume available for the gravity dominated flow. Mazáč et al. (1988) published a pioneering study of concurrent application of geophysical methods and infiltration experiment. Since then, the soil infiltrability of both forest and meadow locations in a number of headwater areas of the Bohemian Forest has been tested.

The present study deals with the results of infiltration experiments conducted at the Liz experimental site (Bohemian Forest, Czech Republic) between years 2003 and 2015. The objective of the research was to assess and compare the spatial and temporal variabilities of the soil infiltrability. For this purpose, a permanent grid of single-ring infiltrometers was established at the experimental site in summer 2003. Since then, ponded infiltration experiments have been conducted every year. In the present paper, temporal instability of the tested soil system is demonstrated together with stepwise changes encountered in the individual infiltration rings. Observed phenomena are discussed in terms of their possible causes. The issues of

experimental shortcomings and general applicability of in-situ ponded infiltration tests are addressed.

MATERIALS AND METHODS

Experimental site

The experimental site Liz is situated on a mildly-sloped meadow next to a meteorological station belonging to the experimental watershed Liz in the Bohemian Forest mountain range, southern Bohemia (Tesař et al., 2006). The altitude of the site is about 830 m above the sea level, the mean annual temperature is 6.3°C, and the mean annual precipitation is 861 mm. The soil is oligotrophic Eutric Cambisol developed upon biotite paragneiss bedrock. Its textural class is coarse sandy loam with clay content less than 1%. Transition to weathered bedrock starts at about 1 m below the surface. The groundwater table is about 8 m below the surface.

Soil water flow character

Results of the dye tracer experiment conducted in 2005 demonstrate the character of soil water flow below infiltration rings at the Liz site (Jelinkova et al., 2006). Water propagates through preferential pathways, while most of the soil profile is bypassed, i.e. does not contribute to water flow. The portion of the soil profile active in the flow process can be approximated by the portion of the soil stained with the dye. The results of the dye tracer experiment are presented in Fig. 1. The dyed portion of the profile (relative to the infiltration ring area) drops fast between the soil surface and the depth of 20 cm to value of about 25%. Between 20 cm and 80 cm below the surface, it grows to about 87%. It drops down to 25% below the depth of 90 cm. The peak at the 80-cm depth is probably related to the transition between the soil and the more compact weathered bedrock.

Experimental setup

In 2003, 17 plastic infiltration rings were installed; 12 in spring and 5 additional in summer (Fig. 2) (Votrubova et al., 2005, 2010). The inner diameter of the rings is 37.5 cm. The insertion depth varies between 10 and 15 cm. In 2005, an additional plastic infiltration ring (No. 18) was installed and used to conduct a dye tracer infiltration followed by excavation (Fig. 1). Also in 2005, a concrete infiltration ring (ring No. 19) with the

same inner diameter was set up for the purpose of monitoring the infiltration process using Electric Resistivity Tomography (Jelinkova et al., 2006). Results of infiltration experiments conducted at this ring are also included in the present study.

Experimental methods

The ponded infiltration experiments were conducted manually. Prior to each experiment, grass within the infiltration ring was cut short and a pin was installed with the pin tip approximately 3 cm above the ground level (± 0.5 cm). This measure, controlling the water pressure at the upper boundary during the infiltration experiment, varied among the infiltration rings and changed between separate infiltrations. The minimum height of the pin tip required is given by the surface elevation differences within the infiltration ring (maximum slope at the experimental site (Fig. 2) is 15%; the rings were installed at spots with lower local slope so that the elevation differences within separate rings did not exceed 3 cm).

Each experiment was started by filling the infiltration ring with water to a level above the pin tip. The volume of this initially applied water varied typically between 3 and 10 liters (recorded approximately with accuracy of about one liter). After that, each time the water surface fell to the level of the pin tip the time was recorded and a 1-litre batch of water was added to the infiltration ring (related water depth variation was 9 mm). Initial decision to conduct the experiments manually was respected throughout the years to maintain consistency.

Generally, each infiltration was continued for two hours or until 40 l of water were infiltrated (excluding the initial batch). This limit was increased to 50 l in 2007–2009. The length of infiltration was decided based on the intent to observe the steady infiltration rate. In 2003–2007, experiments were occasionally terminated earlier when the observed infiltration rate became steady, or due to heavy rain (second-day infiltrations in 2006). In later years, infiltration of 40 liters was not enough to obtain steady infiltration rates; however, a decision was made not to increase the amount of water used in one experiment.

The long-term research consists of separate measurement campaigns comprising infiltration tests in all rings installed. Each campaign was completed within one day. Two separate campaigns with 60-day interval were executed in 2003 (the first one included only 12 infiltration rings) and one in 2004. Each year since 2005, two campaigns have been conducted on two consecutive days. These paired experiments (first-day and

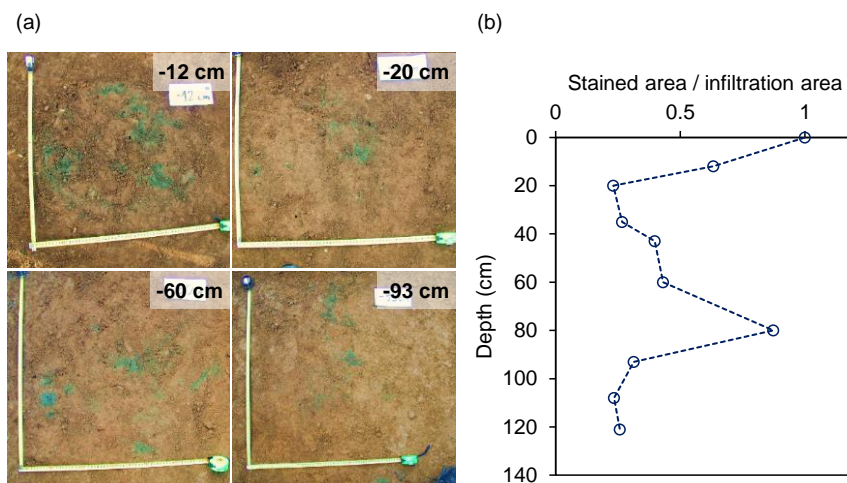


Fig. 1. Results of dye tracer experiment conducted in 2005 (average infiltration rate 14.8 cm h⁻¹, final infiltration rate 12.8 cm h⁻¹): (a) photographs of uncovered profiles at various depths, (b) reconstructed profile of stained-soil fraction relative to the infiltration ring area.

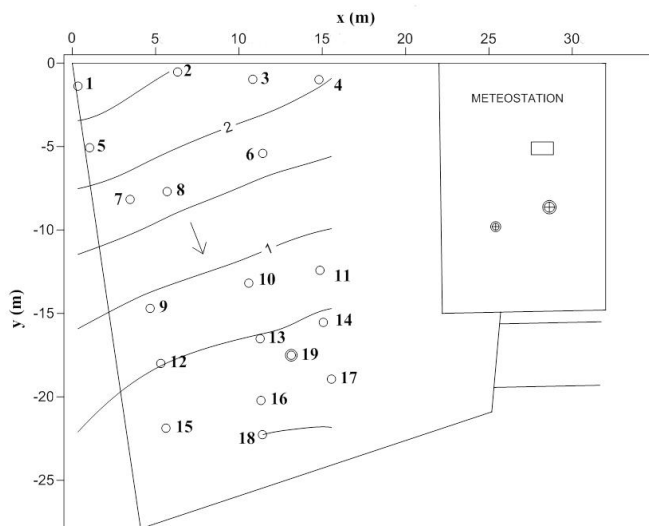


Fig. 2. Map of the experimental site Liz with half-meter elevation contour lines and the established grid of permanent infiltration rings.

second-day infiltrations) can be viewed as the recurrent ponded infiltrations with a one-day interval between the first and the second infiltration runs. In 2005, one more infiltration campaign was conducted 8 days after the second-day infiltration. The results of this campaign were presented in Votrubova et al. (2005); they are not included in the present study.

Data processing

Originally, the observed steady infiltration rate was used to evaluate the infiltrability variations (Votrubova et al., 2005, 2010). However, the character of the infiltration changed dramatically over the years and steady infiltration rates were not always achieved with the limited amount of water infiltrated. Thus, a different quantitative evaluation of the results had to be adopted.

In the present study, estimates of steady state infiltration rate obtained by the extrapolation of the experimental data are evaluated and used in further analyses. For this purpose, the approximation of the infiltration curve based on first two terms of Philip’s expansion (Philip, 1957) was adopted:

$$I = C_1 \sqrt{t} + C_2 t \tag{1}$$

$$i = \frac{C_1}{2\sqrt{t}} + C_2 \tag{2}$$

where t is the time from the start of infiltration (s), I is cumulative infiltration per unit area (m), i is the actual infiltration rate (m s^{-1}), and C_1 and C_2 are optimized parameters ($\text{m s}^{-1/2}$ and m s^{-1} respectively). Assuming linear-in-time effect of lateral flow on cumulative infiltration (Smettem et al., 1994), this approximation can also be used to describe transient infiltration in case of three-dimensional flow below the infiltration ring. An estimate of the transient infiltration rate asymptote is given by the C_2 value. The value of the C_1 coefficient is closely related to the effect of capillary forces and as such is a function of the initial soil water content.

Methods attempting a more rigorous evaluation of the saturated hydraulic conductivity and sorptivity have been developed (Bagarello et al., 2014; Braud et al., 2005; Lassabatère, 2006) based on the infiltration equation presented by Haverkamp et al. (1994). However, apart from assuming homogeneous soil profile with uniform low initial water content, they rely strongly on the Richards type water flow assumption. In our case, the flow is carried by only a portion of the soil profile below the infiltration ring (through preferential pathways). Therefore applicability of these methods is questionable and their results could be misleading. Still, when analyzing variability of the infiltration curves using the parameters C_1 and C_2 , it is instructive to consider their relationship to the well-defined soil hydraulic characteristics, i.e. C_1 is predominantly affected by the soil sorptivity, C_2 by the soil hydraulic conductivity.

Parameter values describing the observed data (i.e. parameters of fitted infiltration curves) were found using differentiated linearization of Eq. (1) (Vandervaere et al., 1997):

$$\frac{dI}{d\sqrt{t}} = C_1 + 2C_2 \sqrt{t} \tag{3}$$

It can be seen that Eq. (1) transforms into the linear relationship between derivative of the cumulative infiltration, $dI / d\sqrt{t}$, and \sqrt{t} . Visualization of data using this transformation provides a simple gauge of how well the data follow the expected behavior expressed by Eq. (2). Example selected from our data is given in Fig. 3.

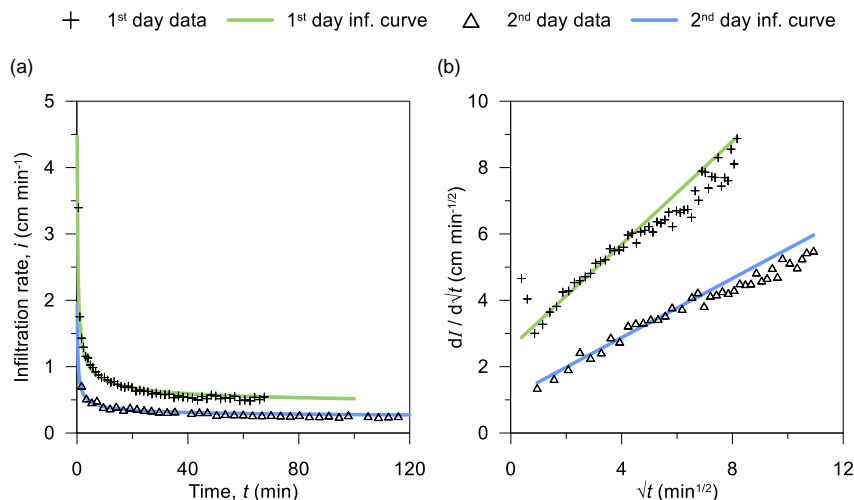


Fig. 3. Infiltration data (ring no. 3, year 2009) and fitted infiltration curves: (a) Actual infiltration rates as a function of time (Eq. (2)), (b) Differential linearization (Eq. (3)).

A slightly concave relationship between the transformed variables was observed (Fig. 3b). This demonstrates discrepancy between the real infiltration process and the theoretical infiltration curve (Eq. (1)). In fact, a distinct change of slope was frequently detected in the linearized projection of the infiltration data. Similar to the results presented in Fig 3, this change was often observed just around the point related to 20th infiltration batch. We assume that it is caused by the wetting front in preferential pathways reaching a less permeable layer of the soil profile that starts about 1 m below the soil surface. Because our main interest lies in the soil profile controlling infiltration under natural conditions, we decided to disregard the later stages of the infiltration. Thus, 20 data points from the beginning of the experiment were generally considered for the infiltration curve fitting. This decision was supported by the fact that the maximum daily rainfall observed at the site since 1976 was 161 mm (recorded on 7/31 1977). Considering the area of the infiltration rings, it corresponds to infiltration of 17.8 liters.

Sometimes, excessive infiltration rates were observed at the very beginning of infiltration (usually during the first-day infiltration). This phenomenon can be noted in Fig. 3b as two outlier points at short times of the first infiltration run. In these cases, the initial data points were omitted from fitting. The phenomenon is also assumed to be related to soil layering (Dohnal et al., 2016); it is probably caused by contrasting hydraulic properties of the upper-most organic layer compared to the main mineral soil profile (the former being more conductive with higher porosity).

To characterize the soil infiltrability by a single number, the time needed to infiltrate a given amount of water can be employed. The limit of 20 liters is used in the present study (chosen arbitrarily) and the quantity is referred to as 20-liter-infiltration time. The volume of the first infiltration batch was approximately evaluated combining extrapolation of the initial data points with information on the total volume of the water batch used to start the experiment and the height of water level maintained in the ring during experiment.

RESULTS AND DISCUSSION

Initial conditions

Data observed at the nearby meteorological station can be used to illustrate soil moisture condition at the experimental site prior the first-day infiltrations. In Fig. 4 the soil water pressure heads at the depth of 25 cm are presented together with the antecedent precipitation within 30 preceding days. Based on these data the experimental sets can be divided into three groups: dry initial conditions (2003a, 2003b, 2010, and 2015), moderate initial conditions (2004, 2007, 2008, 2009, 2011, and 2012), and wet initial conditions (2005, 2006, 2013, and 2014).

Infiltration results overview

An overview of the determined infiltration curve parameters C_2 (i.e. estimated infiltration rate asymptote) and C_1 (i.e. sorptivity related parameter) is presented in Fig. 5. The box plots show the ranges of values obtained for all rings in successive years; results of the first- and the second-day infiltrations are presented separately. An increasing trend is clear for both parameters and both infiltration runs. For C_2 , a distinct stepwise rise of the parameter values can be noted between years 2006 and 2007 as well as between 2012 and 2013. The C_2 values detected during initial years are within the range of expected saturated hydraulic conductivity of sandy loam (or loamy sand).

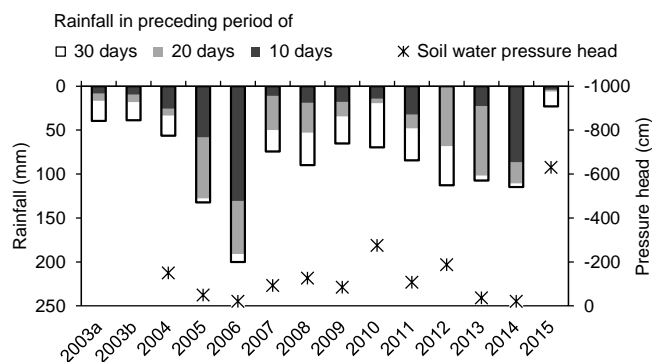


Fig. 4. Initial conditions of the first-day infiltration sets: Antecedent precipitation amount in previous 30 days and the soil water pressure head measured at the depth of 25 cm (not available in 2003).

In final years they reach values common for gravels.

The infiltration rates observed are illustrated by the times at which 20 liters infiltrated (20-liter-infiltration time) presented in Fig. 6 and Table 1. The stepwise change between years 2006 and 2007 is especially pronounced in the first-day infiltration results. Temporal and spatial variability of the results is discussed below.

Second-day infiltration

Generally, a downward shift of the estimated infiltration rate asymptotes, C_2 , between the first and the second infiltration run was observed (Fig. 5). That is in accordance with the previous results of Cislérova et al. (1988). However, cases when it was higher for the second infiltration run were relatively frequent: only in 2009 it did not happen in any ring; in 2010 and 2015 it happened in most rings; and there was no ring in which it would not happen at all.

Considering the other parameter of the fitted infiltration curve, C_1 , it also generally decreases between the two infiltration runs (Fig. 5), which is an expected behavior considering the higher initial soil water content before the second infiltrations. The cases in which this general rule was not obeyed were few (3 in 2006, 2 in 2011, 7 in 2013, and 5 in 2014). They never coincided with the increase of the parameter C_2 .

The results of the second-day infiltrations can be considered as less affected by interannual differences in the initial soil moisture conditions. Still, their temporal variations are similar as observed for the first-day infiltrations, similar increasing trend is obvious in both.

Considering the 20-liter-infiltration time (Fig. 6), as expected, it was longer during the second infiltration runs except 6 isolated occasions. Of these, five coincided with a rise of the estimated infiltration rate asymptote, C_2 , and one with an increase of the sorptivity related parameter, C_1 .

Spatial variability

A weak spatial pattern of increasing infiltrability along the slope can be detected throughout the years. Fig. 7 presents estimated infiltration rate asymptotes, C_2 , for the first-day infiltrations. The results of consecutive campaigns with similar overall results (Fig. 5) are presented separately. Results from all years are presented in Fig. 8 in which the representation of the range of values obtained in individual rings is visualized and

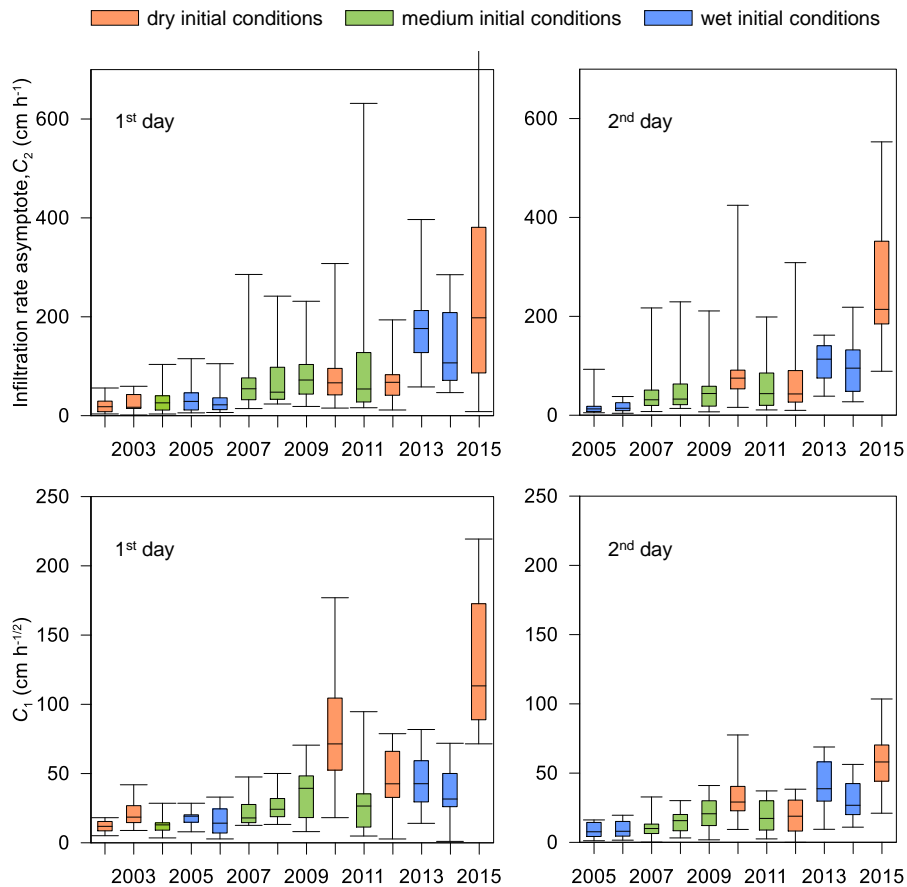


Fig. 5. Parameters of the fitted infiltration curves (C_2 , and C_1 ; Eq. (1)) obtained for all infiltration rings in separate experimental campaigns. Median, quartiles, and extremes are presented for each experimental campaign.

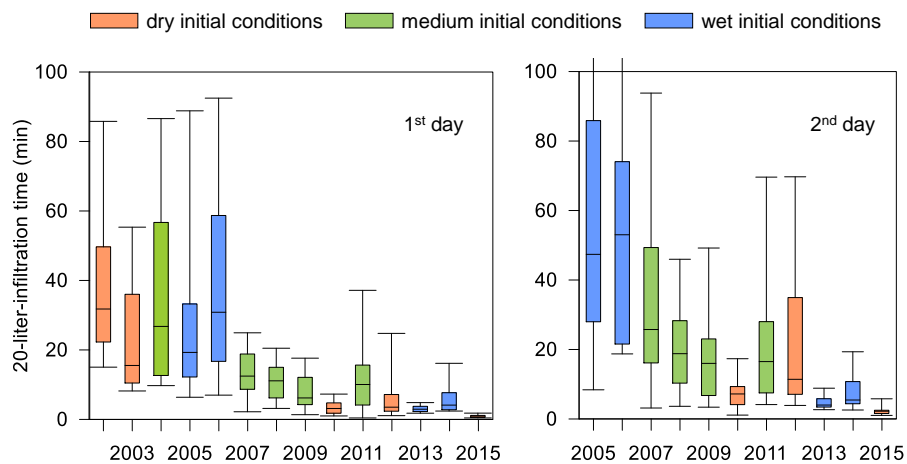


Fig. 6. The time at which 20 liters infiltrated, evaluated for all infiltration rings in separate experimental campaigns. Median, quartiles, and extremes are presented for each experimental campaign.

related to the ring relative elevation. Correlating the ring elevation with extremes and quartiles of all results obtained for each ring, the correlation coefficient ranges from -0.44 to -0.56 for the first-day infiltrations, and from -0.24 to -0.47 for the second-day infiltrations. Considering each infiltration campaign separately, the correlation coefficients between the ring elevation and the estimated infiltration rate asymptotes are negative in all cases (between -0.07 and -0.52 for the first-day infiltrations, and between -0.02 and -0.50 for the second day infiltrations) except second-day infiltrations in 2012. The prevalence of negative values signals the persistence of the trend. The

variability between years reflects a considerable disorder in the temporal changes observed in different infiltration rings.

For an idealized system with homogeneous soil without preferential flow, the effect of differences in the ring insertion and in the ponding depth on the estimated infiltration rate asymptote, C_2 , can be evaluated (Dusek et al., 2009; Reynolds and Elrick, 1990). For the ring insertion between 10 and 15 cm and the ponding depth between 20 and 40 mm, the related variability in detected C_2 would be less than 15%. The variability of the results encountered in our study exceeds this level significantly (Table 1).

Table 1. Time at which 20 liters infiltrated: (a) the first day infiltrations, (b) the second day infiltrations. Color intensity highlights differences (categories below 20, 10, and 3 minutes are marked with increasing color intensity). Empty cells with high color intensity represent instances when the infiltration was too fast to be measured. White empty cells denote that the experiment was not conducted.

(a)

20-liter-infiltration time (min), first-day infiltration sets														
Ring	2003a	2003b	2004	2005	2006	2007	2008	2009	2010	2011	2012	2013	2014	2015
1	21	10	26	28	36	20	17	17	3	7	2	4	3	1
2	33	13	60	36	62	16	11	13	4	14	3	3	8	1
3	36	36	64	33	59	24	18	18	5	26	10	3	7	<0.5
4	50	12	87	43	91	25	11	15	3	15	3	4	2	1
5	86	45	39	89	92	22	12	5	4	7	7	3	4	1
6	15	12	10	6	31	17	12	12	7	10	25	4	16	2
7	31	13	34	14	16	6	5	6	3	10	10	4	8	1
8	37	8	11		33	12	7	6	3	16	7	3	6	2
9		26	13	15	28	9	6	6	5	0	2	2	3	1
10		55	20	12	17	9	4	4	2	5	3	2	4	1
11	22	9	21	15	25	10	17	8	2	37	4	3	4	1
12		30		23	12	2	20	5	1	3	2	3	4	1
13		45	54	31	50	15	10	4	3	18	7	3	8	1
14		18	27	8	17	6	6	3	1	4	1	2	3	<0.5
15	22	10	23	15	30	13	12	4	2	4	3	2	3	1
16	23		12		7	6	3	1	1	4	2	3	2	1
17	83	26	57	31	61	19	15	9	6	29	9	2	8	1
19				9	11	9	11	11	6	16	5	5	13	2

(b)

20-liter-infiltration time (min), second-day infiltration sets														
Ring	2003a	2003b	2004	2005	2006	2007	2008	2009	2010	2011	2012	2013	2014	2015
1				70	62	44	40	44	7	8	4	6	4	2
2				86	81	55	13	24	9	17	11	3	10	2
3				113	86	94	46	49	12	55	70	5	11	2
4				93	73	87	18	31	7	22	8	4	3	2
5				short	107	57	25	7	6	11	17	5	5	3
6				8	27	28	10	18	8	18	44	6	19	4
7				28	22	11	7	11	4	22	39	8	11	1
8					short	24	13	14	7	16	31	8	6	3
9				27	44	17	14	18	9		7	4	3	2
10				23	19	27	8	8	4	8	12	4	5	2
11				37	31	25	42	22	6	70	4	4	5	2
12				46	short	3	24	7	1	4	10	3	4	2
13				122	73	29	24	12	8	31	15	4	10	2
14				53	21	16	10	6	4	6	6	3	4	1
15				38		18	20	6		6	7	3	3	1
16						7	4	3		4	4	4	3	1
17				49	74	49	28	21	16	28	36	3	11	3
19					21	15	30	23	17	20	35	9	18	6

Temporal variability in general

Generally, the infiltrability observed in the grid of permanent infiltration rings increased throughout the years. Considering the estimated infiltration rate asymptotes (Fig. 5), stepwise changes between years 2006 and 2007 as well as between 2012 and 2013 can be noted. Different character of changes is found if the 20-liter infiltration times are examined (Fig. 6). Although the stepwise decrease after 2006 can be noted too, the following

evolution can be described rather as a decrease with fluctuations.

Confrontation of the infiltration results with the interannual changes of the initial soil moisture conditions (Figs. 4, 5, 6) discloses no general relationship between the infiltration character and the soil initial moisture conditions. It can be seen that the estimated infiltration rate asymptote, C_2 , rises irrespective of the changes in the initial soil moisture status. Considering the sorptivity related C_1 parameter, a similar increase in time is

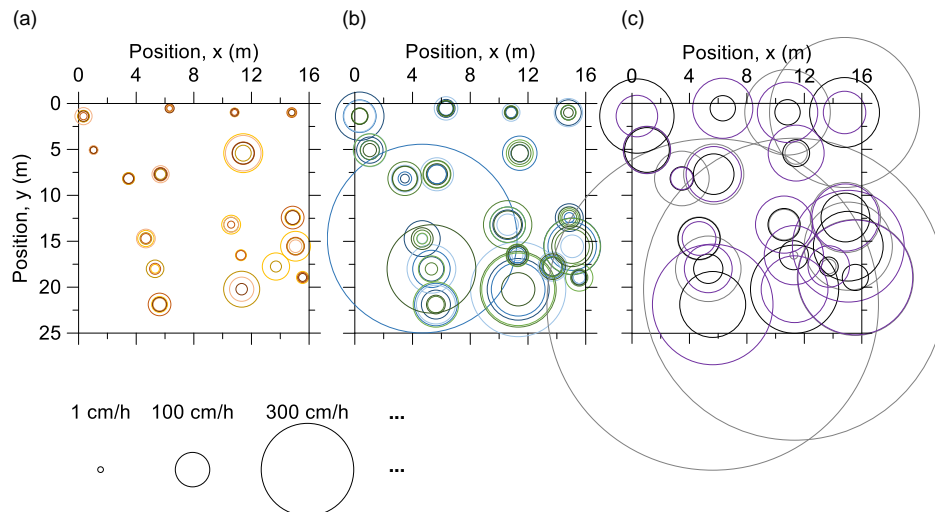


Fig. 7. Spatial distribution of the estimated infiltration rate asymptotes, C_2 , obtained for the first-day infiltrations in consecutive years: (a) 2003–2006, (b) 2007–2012, and (c) 2013–2015. Diameters of the circles are linearly proportional to the C_2 values being depicted as indicated. Spatial coordinate system corresponds to that in Fig. 2. Individual infiltration campaigns are denoted with different colors (see Fig. 8 for details).

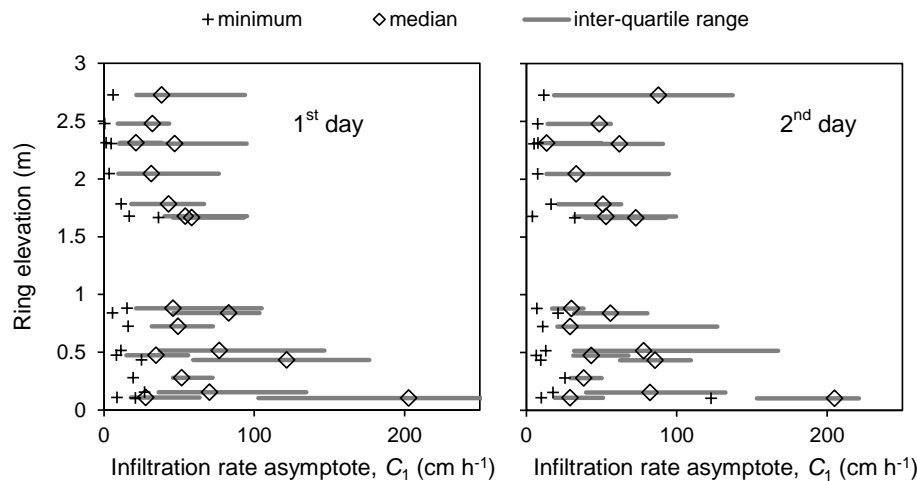


Fig. 8. Relationship between the ring relative elevation and the infiltration rate asymptotes, C_2 , detected for the first- and the second-day infiltrations.

combined with local rises in years with dry initial conditions (2010, 2015). A corresponding gradual decrease with local extremes can be noticed in the plot of 20-liter-infiltration time. This reaction to the dry initial conditions is in accord with the effect of the initial conditions on the soil sorptivity (the lower the water content, the higher the soil sorptivity and faster the initial infiltration rates). On the whole, however, the results do not follow such trend consistently. The obvious shift in results obtained in years with relatively similar initial moisture condition (compare results obtained for dry initial conditions, or for wet initial conditions) indicates instability of the system tested.

After the gradual interannual infiltration rate increase was detected, a possible impact of the experimental setup and unnatural amount of water infiltrated was hypothesized. Therefore an additional infiltration was conducted in a temporarily installed infiltration ring in 2010. The obtained estimated infiltration rate asymptote (34 cm h^{-1}) was the fourth lowest out of the results of the first day infiltrations. Thus, the hypothesis was not clearly supported and the natural temporal evolution of the soil profile infiltration properties was not ruled out. After further increase of the observed infiltration rates, two additional

control infiltrations were conducted in 2014. The obtained estimated infiltration rate asymptotes stayed similar as in 2010 (41 cm h^{-1} , and 30 cm h^{-1}) and the results for all the permanent rings were considerably higher (similar results were obtained for the infiltration ring No. 19 (made of concrete)). All results obtained in temporarily installed rings lie between the third quartile and the maximum of the values obtained in the first experimental set in 2003. The fact that the control infiltrations are at the faster end of the infiltration rates observed during the initial experimental campaign can be a consequence of the soil distortion during ring installation (while the permanent infiltration rings were installed several days prior the first infiltration experiment, the temporal infiltration rings were installed just before the experiment).

Temporal variability in separate infiltration rings

An interesting phenomenon can be seen when infiltration curves observed in a certain ring in different years are confronted (Fig. 9). The general trend of the interannual changes is from lower to higher infiltration rates. This increase is not

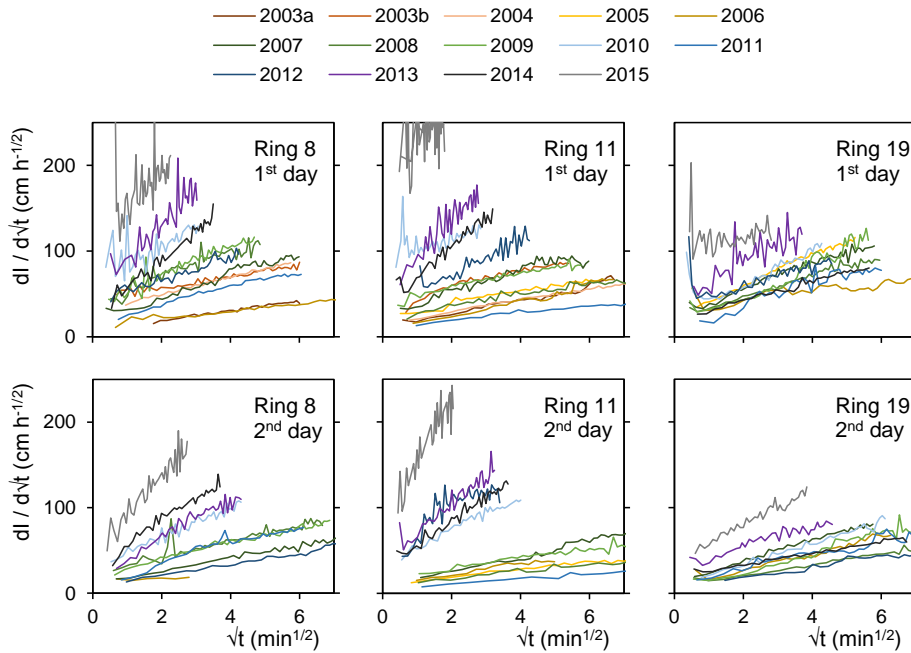


Fig. 9. Infiltration curves observed in three selected infiltration rings in different years during either the first-day infiltration or the second-day infiltration (linearization according to Eq. (3) is employed; the slope of the infiltration lines serves as an estimate of the infiltration rate asymptote).

monotonous; the infiltration curves in successive years switch up or down between apparently stable infiltration modes. This behavior was observed for both the first-day and the second-day infiltrations in the majority of infiltration rings. Similarity between certain years in respect to the first-day infiltration curves is sometimes accompanied by alike similarity in respect to the second-day infiltration curves (2008 and 2009 in Ring 8, 2007 and 2009 in Ring 11, or 2005 and 2007 in Ring 11). However, as can be seen in Fig. 9, such behavior is not a general rule.

It is worth mentioning that the temporally most stable results were obtained for the concrete infiltration ring, ring no. 19 (relative elevation 0.28 m in Fig. 8), which are also presented in Fig. 9. Two reoccurring infiltration modes are notable for the first-day infiltrations (indicating the infiltration rate asymptote at about 50 cm h^{-1} and 75 cm h^{-1}). Three reoccurring infiltration modes can be seen in the second-day results (indicating infiltration rate asymptotes at 26 cm h^{-1} , 38 cm h^{-1} , and 49 cm h^{-1}). Even in this ring, the interannual infiltration rate changes are not related to the initial soil moisture conditions and progressively higher infiltration rates were observed in later years (2013 and 2015). The reason why the extreme values are notably lower than in all other rings may be related to the fact, that this infiltration ring was installed later (in 2005).

Possible sources of detected infiltration instability

Considering the presented character of soil water flow (i.e. preferential flow demonstrated by the dye-tracer experiment), the interannual switching between seemingly stable infiltration modes may be explained by variable activation of otherwise stable preferential pathways. The potential preferential pathways are determined by the soil profile internal structure that is stable in time. The actual activation of the pathways is controlled by the soil properties and conditions near the upper boundary (the surface layer of the soil profile).

A possible impact of the vast amount of water infiltrated each year at the same spots need to be considered (over 725 mm of water are infiltrated in two infiltrations runs, which corresponds to 84% of the mean annual precipitation at the site). It could possibly lead to gradual increase of the hydraulic conductivity of the system due to fine particles displacement. However, the fluctuations between distinct stable infiltration modes described above do not support this. Moreover, the extent of the infiltration rates increase would indicate more radical changes of the soil structure.

Gradual occurrence of extremely high infiltration rates could be related to the activity of burrowing animals, including both invertebrates, like worms or ants and other insects, and small mammals, like rodents, shrews or moles. Although no objective record have been kept, the amount of visible burrows at the experimental site seems to be increasing. Naturally, the biological activity was present prior to the setting up the infiltration rings, however, the burrows were distributed randomly and their horizontal connectivity disrupted by the ring insertion (within the upper 10 cm). After the rings were installed, gradual establishment of deeper burrows connecting the inside of the ring with the surroundings may have taken place. In this regard, the animal preference for the place inside and/or near the installed infiltration ring cannot be ruled out. It should be noted that the surface inside the infiltration rings were inspected prior the infiltration and all burrows reaching the soil surface were plugged with stones and soil mixture. Still, it is possible that under the positive water pressure applied at the soil surface, the burrows beneath the surface (even without an obvious connection to the soil surface) could get filled and conduct the water. In few cases, borrow opening became obvious after the start of the infiltration, in which cases the experiment was stopped.

It should be also noted, that the year 2002 (i.e. the year before the onset of the study) was the wettest year on record (since 1976); also three out of ten days with maximum daily precipitation amount on record were observed in 2002. The extreme character of the year 2002 could cause reduction of

burrowing mammals' population at the site. The last year of the study, 2015, was actually the driest year on record.

The fact that the most temporally stable results were obtained for the concrete infiltration ring may imply that the ring material affects the results (concrete ring is subject to less volumetric changes due to temperature variations than the plastic rings). On the other hand, it may be related to the later installation of this ring or it can be just a coincidence.

The character of the detected temporal changes was a subject of a simulation study using a Richards-equation based dual-continuum model (Dohnal et al., 2016). Various scenarios of possible changes of the soil profile were tested. Only a scenario with increased conductivity of surface organic layer combined with large sink hole and significant volume of preferential pathways was able to reproduce infiltration rates comparable to those observed in later years of the long-term experimental study presented in this paper.

CONCLUSIONS

A long-term testing of soil infiltrability was performed in a grid of 18 permanent infiltration rings. Pondered infiltration experiments were conducted annually between 2003 and 2015. The original intent of the study was to assess the spatial and temporal variability of the soil hydraulic properties.

The encountered temporal changes of infiltration rates observed vastly overrode the spatial variability observed during initial years. However, when only initial years until 2006 are considered, the temporal variability of the infiltration rates observed in individual rings is generally less than the spatial variability among the rings in individual years. Perhaps, the fact that temporal variability becomes greater than the spatial variability indicates changes of the soil profile induced by external factors.

The main character of the temporal changes can be described as switching between relatively stable infiltration modes. This behavior is probably related to variable activation of preferential pathways within the soil profile. While the pathways themselves are probably stable in time, the overlying surface layer of the soil is changing (reflecting changing meteorological conditions and animal activity) and consequently the portion of the pathways that become active during an infiltration event may vary. The reoccurrence of certain infiltration modes was detected for infiltrations at both ends of the range of infiltration rates observed.

The extreme infiltration rates observed in later years together with the contrasting results obtained in temporally installed rings in 2010 and 2014 lead to a conclusion that the results are affected by the animal activity at the experimental plot and the experimental procedure employed. Perhaps the large amount of water infiltrated during an experiment may lead to stabilization of once activated flow paths and their easier activation during next infiltration events and possibly even to an increase in their conductivity. In view of our results, repeated pondered infiltration in stable infiltration rings may provide valuable information on the temporal variability of the soil infiltrability, providing the possible impact of burrowing animals is taken into account and the volume of water used in experiments does not exceed reasonable amounts for the soil under study.

Acknowledgements. The study was funded by the Czech Science Foundation, project No. 16-05665S. The extensive experimental work would not have been possible without the kind support and help of many Mgr and PhD students and faculty members from CTU in Prague.

REFERENCES

- Angulo-Jaramillo, R., Thony, J.L., Vachaud, G., Moreno, F., Fernández Boy, M.E., Cayuela, J.A., Clothier, B.E., 1997. Seasonal variation of hydraulic properties of soils measured using a tension disk infiltrometer. *Soil Sci. Soc. Am. J.*, 61, 1, 27–32.
- Bagarello, V., Sgroi, A., 2004. Using the single-ring infiltrometer method to detect temporal changes in surface soil field-saturated hydraulic conductivity. *Soil & Tillage Research*, 76, 1, 13–24.
- Braud, I., De Condappa, D., Soria, J.M., Haverkamp, R., Angulo-Jaramillo, R., Galle, S., Vauclin, M., 2005. Use of scaled forms of the infiltration equation for the estimation of unsaturated soil hydraulic properties (the Beerkan method). *Eur. J. Soil Sci.*, 56, 3, 361–374
- Cislerova, M., Simunek, J., Vogel, T., 1988. Changes of steady-state infiltration rates in recurrent ponding infiltration experiment. *J. Hydrol.*, 104, 1–16.
- Dohnal, M., Vogel, T., Dusek, J., Votrubova, J., Tesar, M., 2016. Interpretation of ponded infiltration data using numerical experiments. *J. Hydrol. Hydromech.*, 64, 3, 289–299.
- Dusek, J., Dohnal, M., Vogel, T., 2009. Numerical analysis of ponded infiltration experiment under different experimental conditions. *Soil & Water Res.*, 4, S22–S27.
- Ferreira, C.S.S., Walsh, R.P.D., Steenhuis, T.S., Shakesby, R.A., Nunes, J.P.N., Coelho, C.O.A., Ferreira, A.J.D. 2015. Spatiotemporal variability of hydrologic soil properties and the implications for overland flow and land management in a peri-urban Mediterranean catchment. *J. Hydrol.*, 525, 249–263.
- Gomi, T., Sidle, R.C., Miyata, S., Kosugi, K., Onda, Y., 2008. Dynamic runoff connectivity of overland flow on steep forested hillslopes: Scale effects and runoff transfer. *Water Resour. Res.*, 44, W08411. DOI:10.1029/2007WR005894.
- Haverkamp, R., Ross, P.J., Smettem, K.R.J., Parlange, J.-Y., 1994. Three dimensional analysis of infiltration from the disc infiltrometer: 2. Physically-based infiltration equation. *Water Resour. Res.*, 30, 2931–2935.
- Hu, W., Shao, M., Wang, Q., Fan, J., Horton, R., 2009. Temporal changes of soil hydraulic properties under different land uses. *Geoderma*, 149, 355–366.
- Jelinkova, V., Votrubova, J., Sanda, M., Cislerova, M., 2006. Monitoring preferential flow during infiltration experiments. *Eos Trans. AGU*, 87, 52, Fall Meet. Suppl., Abstract H31B-1419.
- Johnson, A.I., 1963. A field method for measurement of infiltration. General ground-water techniques. Geological Survey Water-Supply Paper 1544-f. United States Government Printing Office, Washington, D.C., USA.
- Kargas, G., Kerkidesa, P., Sotirakoglou, K., Poulouvassilis, A., 2016. Temporal variability of surface soil hydraulic properties under various tillage systems. *Soil & Tillage Research*, 158, 22–31.
- Lassabatère, L., Angulo-Jaramillo, R., Ugalde, J.M.S., Cuenca, R., Braud, I., Haverkamp, R., 2006. Beerkan estimation of soil transfer parameters through infiltration experiments – BEST. *Soil Sci. Soc. Am. J.*, 70, 2, 521–532.
- Ma, L., Hoogenboom, G., Saseendran, S.A., Bartling, P.N.S., Ahuja, L.R., Green, T.R., 2009. Effects of estimating soil hydraulic properties and root growth factor on soil water balance and crop production. *Agron. J.*, 101, 572–583.
- Mazáč, O., Cislerová, M., Vogel, T., 1988. Application of geophysical methods in describing spatial variability of saturated hydraulic conductivity in the zone of aeration. *J. Hydrol.*, 103, 117–126.

- Philip, J.R., 1957. The theory of infiltration: 4. Sorptivity and algebraic infiltration equations. *Soil Sci.*, 84, 257–284.
- Reynolds, W.D., Elrick, D.E., 1990. Ponded infiltration from a single ring: I. Analysis of steady flow. *Soil Sci. Soc. Am. J.*, 54, 1233–1241.
- Sharma, M.L., Gander, G.A., Hunt, C.G., 1980. Spatial variability of infiltration in a watershed. *J. Hydrol.*, 45, 101–122.
- Smettem, K.R.J., Parlange, J.-Y., Ross, P.J., Haverkamp, R., 1994. Three dimensional analysis of infiltration from the disc infiltrometer: 1. A capillary based theory. *Water Resour. Res.*, 30, 2925–2929.
- Starr, J.L., 1990. Spatial and temporal variation of ponded infiltration. *Soil Sci. Soc. Am. J.*, 54, 3, 629–636.
- Šimůnek, J., 1988. Infiltration – numerical simulation. *Vodohospodářský Časopis*, 36, 407–420. (In Czech.)
- Tesař, M., Balek, J., Šír, M., 2006. Hydrological research in the Volyňka basin (Bohemian Forest, Czech Republic). *J. Hydrol. Hydromech.*, 54, 137–150. (In Czech with English resumé.)
- Vandervaere, J.-P., Peugeot, C., Vauclin, M., Angulo-Jaramillo, R., Lebel, T., 1997. Estimating hydraulic conductivity of crusted soils using disc infiltrometers and minitensiometers. *J. Hydrol.*, 188–189, 203–223.
- Votrubova, J., Jelinkova, V., Cislerova, M., Tesar, M., 2005. Infiltration capacity of soils on experimental site Liz (Sumava Mountains). In: Workshop Adolfa Patery 2005 - Extrémní hydrologické jevy v povodích. Czech Technical University, Prague, pp. 205–216. ISBN 80-01-03325-2.
- Votrubova, J., Jelinkova, V., Nemcova, R., Tesar, M., Vogel, T., Cislerova, M., 2010. The soil apparent infiltrability observed with ponded infiltration experiment in a permanent grid of infiltration rings. *Geophysical Research Abstracts*, Vol. 12, EGU2010-11898.

Received 15 July 2016
Accepted 30 January 2017